MILCOM 2024 - 2024 IEEE Military Communications Conference (MILCOM) | 979-8-3503-7423-0/24/$31.00 ©2024 IEEE | DOI: 10.1109/MILCOM61039.2024.10773626

An Improved Weight Selection Algorithm for Interference Mitigation in Paraboloidal Reflector Antennas with Reconfigurable Rim Scattering

Xinrui Li, R. Michael Buehrer, Steven W. Ellingson
Bradley Department of Electrical and Computer Engineering
Virginia Tech, Blacksburg, VA, 24061, USA
{lxinrui3, rbuehrer, ellingso}@vt.edu

***Abstract*—With the explosion of proposed LEO satellite systems and constellation sizes, the potential benefits of spectrum sharing for satellite-based systems has increased tremendously. Our previous work has demonstrated that modifying the rim scattering of a paraboloidal reflector antenna using reconfigurable elements allows for interference cancellation [1], [2]. However, for dynamic spectrum sharing there is a need for algorithms with faster convergence and improved performance. Thus, in this work we develop improved algorithms for determining the weights of such a receiver system which could serve as the basis of a spectrum sharing approach. We begin this work by reviewing the unconstrained optimal weight values needed at each reconfigurable element for interference mitigation as well as the previously proposed approach for finding a unimodular solution. We then show that near-optimal unimodular weights can be found in closed form provided that the unconstrained optimal weight vector has an infinite norm that does not exceed unity. In such case, the near-optimal continuous phase unimodular weights can be determined with significantly lower complexity while still providing acceptable attenuation at the desired angles. Next, in order to find weights with discrete phase values (to simplify implementation), we transform the original problem using a penalty method and solve it by leveraging the Majorize-Minimization (MM) algorithm. It is shown that this algorithm converges significantly faster and provides deeper nulls than the previously proposed simulated annealing approach. Further, based on empirical results, we provide a simple criterion for the existence of unimodular weights which provide perfect nulls for all desired angles. Finally, we numerically demonstrate the convergence and gain values provided by the proposed algorithms are superior to previously proposed algorithms.**

***Index Terms*—Reconfigurable antennas, reconfigurable intelligent surfaces, unit-modulus least squares, constant modulus optimization.**

I. Introduction

There has been a recent push for the expansion of the use of Low Earth Orbit (LEO) satellites (including mega-constellations) for communication systems and other purposes [3]. New wireless systems lead to the need for spectrum, and as a result, the investigation of spectrum sharing between existing systems (e.g., Geosynchronous Earth Orbit (GEO) satellite systems) and LEO systems [4]. In a spectrum sharing scenario between existing GEO and new LEO networks, the LEO satellite systems will have to protect the existing GEO systems, possibly by constructing protection areas [4]. However, given the expected growth in the size and number of LEO satellite constellations it is not clear that such an approach scales well. GEO satellites are used for various purposes including communications, weather monitoring, earth observation and navigation services [5]–[7]. Large reflector antennas are often deployed at GEO earth stations in such systems. Thus, interference mitigation approaches for these antennas should prove to be beneficial for spectrum sharing [8].

Recently, an approach for cancelling (or generally modifying) the sidelobe(s) of a reflector antenna pattern has been proposed that uses reconfigurable rim scattering [1]. In this approach, the rim of a reflector antenna is equipped with reconfigurable elements which are capable of introducing a phase shift to the reflected signal. As a result, the sidelobes of the pattern can be altered and even cancelled, which can potentially improve the efficiency of spectrum sharing. Such reconfigurable elements are nearly-passive devices made of electromagnetic materials which can be reconfigured by tuning the surface impedance through various mechanisms and therefore can be deployed on the structures of the reflector antenna at low-cost [9]. Moreover, the authors in [10] presented a practical design for such a reconfigurable antenna and demonstrated the efficacy of this concept through full-wave simulation.

In the current work we build on the system model proposed in [1], describe new algorithms for determining the complex weights needed at each reconfigurable element to cancel sidelobes at specific angles from the reflector axis and comparing the results to those described in [2], [11]. We first derive the optimal weights needed to cancel sidelobes at an arbitrary angle ψ. In order to reduce the implementation cost and complexity, the weights are generally restricted to constant-modulus in practice. For constant-modulus weights, the optimal weight vector can be determined by formulating a unit-modulus least squares (UMLS) problem. A UMLS problem is a non-convex problem due to the unit-modulus constraint. When the dimension of the problem is small, the problem can be solved

This work was supported in part by the National Science Foundation under Grant AST-2128506.

using the semidefinite relaxation (SDR) algorithm [12]. SDR converts the problem into a convex problem by dropping the rank one constraint and the solution for the original problem can be retrieved through randomization of the solution for the relaxed problem. The author in [13] proposed a phase-only conjugate gradient and phase-only Newton's method which optimize over the phase variable of the weight vector. On the other hand, for large scale problem considered in this paper, the projected gradient method is a promising solution due to its low computational complexity and its convergence properties which are discussed in [14] and [15]. Moreover, by utilizing the properties specifically from our problem, a closed form expression for approximately optimal unimodular weights is derived. This solution provides excellent performance while demonstrating significantly lower computational complexity than any of the proposed iterative algorithms.

Further, we transform the problem using a penalty method and employ a majorization minimization method which determines weights that are both unimodular and discrete phase. This approach appears to be significantly superior (both in complexity and performance) relative to previously proposed approaches. While the existing literature dealing with the unit-modulus least squares (UMLS) problems pays significant attention to the minimization of the objective function, the conditions under which there exists a unimodular solution that minimizes the objective function to zero have not been fully investigated. Using empirical results, we find a simple criterion for determining the existence of unimodular weights which strictly meet optimality criterion, and demonstrate the validity of this criterion through simulations.

This paper is organized as follows: Section II describes the system model used in this work. Section III presents the methods for determining the optimal weights under various constraints. In particular, we start with unconstrained weights and then review the Gradient Projection algorithm for finding the unimodular weights with continuous phase. Additionally, we find a closed-form solution for unimodular weights that are near-optimal, but only exist if the infinite norm of the optimal weights is less than unity. We then transform the problem through penalty method and deploy an algorithm through majorization minimization method which determines weights that are both unimodular and discrete phase. Section IV presents the criterion for determining the existence of the unimodular weights which strictly satisfy the linear equality. Section V provides numerical results which characterize the performance of the proposed algorithms. Subsequently, section VI concludes the paper.

II. System Model

The antenna system assumed in this paper is presented in Fig. 1. Following the development in [1], we assume the equivalence of transmit and receive patterns and calculate the transmit patterns using physical optics (PO). The total electric field intensity $\mathbf{E}^s$ scattered by the reflector in the far-field direction ψ is given by

$$\mathbf{E}^s(\psi) = \mathbf{E}_f^s(\psi) + \mathbf{E}_r^s(\psi), \tag{1}$$

where $\mathbf{E}_f^s$ is the electric field intensity due to the fixed portion of the dish in the direction ψ and $\mathbf{E}_r^s$ is due to the reconfigurable portion of the dish. See the system settings in [1], [11] for details. Due to the discrete nature of the reconfigurable surface, we can write $\mathbf{E}_r^s(\psi)$ as

$$\mathbf{E}_r^s(\psi) = -j\omega\mu_0 \frac{e^{-j\beta r}}{4\pi r} \sum_n \mathbf{J}_1\left(\mathbf{s}_n^i\right) e^{j\beta\hat{\mathbf{r}}(\psi)\cdot\mathbf{s}_n^i} \Delta s, \tag{2}$$

where the summation is made over all the reconfigurable elements, $j = \sqrt{-1}$, ω is the operating frequency in rad/s, μ_0 is the permeability of free space, β is the wavenumber, $\hat{\mathbf{r}}(\psi)$ points from the global origin towards the field point in the direction ψ. $\mathbf{J}_1\left(\mathbf{s}_n^i\right) = w_n \mathbf{J}_0\left(\mathbf{s}_n^i\right)$ is the current distribution due to the n-th element with complex-valued weight w_n, where $\mathbf{J}_0(\mathbf{s}^i)$ is the PO equivalent surface current distribution. These weights will be designed to cancel sidelobes in the H-plane co-pol pattern. Thus, we are primarily concerned with the y-component of the vector $\mathbf{E}_r^s(\psi)$ and define the complex scalar $E_r^{s,co}(\psi)$ to be the y-component of the vector $\mathbf{E}_r^s(\psi)$. Also, for convenience, we can write $E_r^{s,co}(\psi)$ in terms of two $N \times 1$ dimensional arrays $\mathbf{e}_\psi$ and $\mathbf{w}$ representing the co-pol portion of the electric field intensity without the influence of the elements and the complex-valued element gains respectively:

$$E_r^{s,co}(\psi) = \mathbf{e}_\psi^T \mathbf{w}, \tag{3}$$

where $\mathbf{x}^T$ is the transpose of the vector $\mathbf{x}$ and the n-th element of $\mathbf{e}_\psi$ is

$$e_{\psi,n} = \left(-j\omega\mu_0 \frac{e^{-j\beta r}}{4\pi r} \mathbf{J}_0\left(\mathbf{s}_n^i\right) e^{j\beta\hat{\mathbf{r}}(\psi)\cdot\mathbf{s}_n^i} \Delta s\right) \cdot \hat{\mathbf{y}}, \tag{4}$$

where the operation $(\mathbf{e}) \cdot \hat{\mathbf{y}}$ selects the y-component of the vector $\mathbf{e}$. Note that both one-dimensional arrays are of length N where N is equal to the number of reconfigurable elements placed along the rim of the dish.

Now to cancel the sidelobe gainat angle ψ, we wish

$$E_f^{s,co}(\psi) + E_r^{s,co}(\psi) = 0. \tag{5}$$

Thus, we wish to find the set of optimal weights $\mathbf{w}^*$ such that

$$\mathbf{e}_\psi^T \mathbf{w}^* = -E_f^{s,co}(\psi). \tag{6}$$

Similarly, if we consider the case of K desired nulls at K different angles, we can re-write the problem as

$$\mathbf{A}\mathbf{w}^* = \mathbf{y}, \tag{7}$$

where

$$\begin{aligned} \mathbf{A} &= \left[\mathbf{e}_{\psi_1}, \cdots, \mathbf{e}_{\psi_K}\right]^T \in \mathbb{C}^{K\times N}, \\ \mathbf{y} &= -\left[E_f^{s,co}(\psi_1), \ldots, E_f^{s,co}(\psi_K)\right]^T \in \mathbb{C}^{K\times 1}. \end{aligned} \tag{8}$$

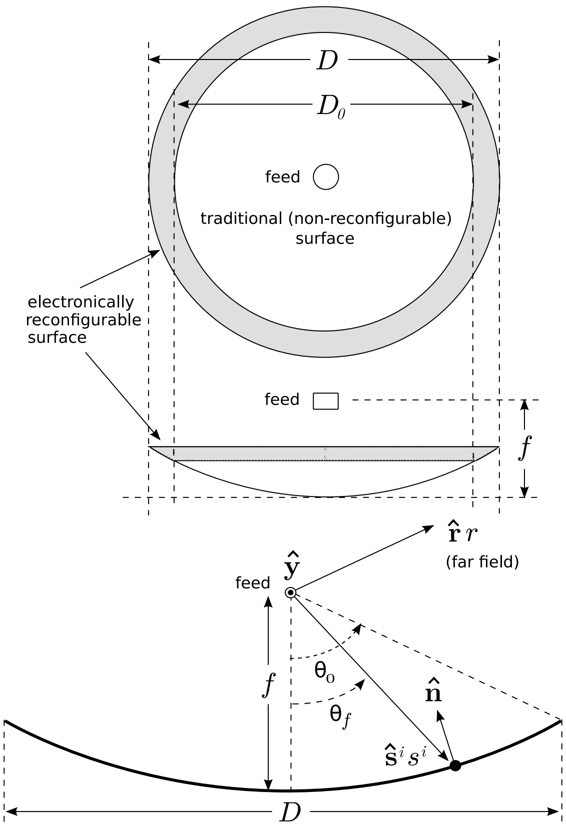

Fig. 1. On-axis (top) view of an electronically- reconfigurable rim scattering system assumed in this paper. The global origin is defined as the bottom of the dish. θ_f is the angle measured from the reflector axis of rotation toward the rim with $\theta_f = \theta_1$ at the rim of the fixed portion of the dish and $\theta_f = \theta_0$ at the rim of the entire dish, ϕ is the angular coordinate orthogonal to both θ_f and the reflector axis.

Moreover, if we want to avoid variation in the mainlobe, we can include a constraint for the mainlobe. Specifically, for $\psi = 0°$, we require $\mathbf{e}_0^T \mathbf{w}^* = \kappa$,, where κ is the target constraint. Ideally, we could set $\kappa = \mathbf{e}_0^T \mathbf{1}$, which provides the same mainlobe gain as the 18m fixed reflector. However, with weights restricted to unit modulus, satisfying both the mainlobe constraint and side lobe constraints may not be possible. One option is to ease the constraints by choosing κ = 0, which equals to the mainlobe gain provided by a 17m fixed dish, although this removes any contribution of the reconfigurable portion of the reflector to the mainlobe. Alternatively, we could choose $\kappa = \delta E_f^{s,co}(0)$, for some small value δ to provide some additional gain in the mainlobe from the perspective of a 17m fixed dish. Experimentally we have found this latter approach to be successful. Thus, we can modify the vector of requirements to be

$$\begin{aligned} \mathbf{A} &= \left[\mathbf{e}_{\psi_0}, \mathbf{e}_{\psi_1}, \cdots, \mathbf{e}_{\psi_K}\right]^T, \\ \mathbf{y} &= -\left[-\delta E_f^{s,co}(0), E_f^{s,co}(\psi_1), \ldots, E_f^{s,co}(\psi_K)\right]^T. \end{aligned} \tag{9}$$

In the following section we describe techniques to determine the optimal weights with different constraints.

III. Weight Selection

As discussed in [2], the approach to find the appropriate weights which satisfy (7) depends on the restrictions placed on $\mathbf{w}^*$. First, we describe how to determine the weights with no restrictions placed on $\mathbf{w}^*$. Second, we will describe techniques for finding $\mathbf{w}^*$ if the weights are restricted to unit-modulus values (i.e., phase-shifting only). Finally, we describe approaches to find the weight vector if we further restrict the phase to be discrete (i.e., come from a finite set).

A. Unquantized Weights

If the weights are unconstrained, to form a null at all desired angles, we can simply let $\mathbf{w}^*$ be equal to

$$\mathbf{w}^* = \mathbf{A}^H \left(\mathbf{A}\mathbf{A}^H\right)^{-1} \mathbf{y}. \tag{10}$$

We will term this as the unconstrained optimal weights since these weights guarantee that the response of the dish in the direction ψ is zero. Unfortunately, $\mathbf{w}^*$ in general has elements with $|w_n| \neq 1$ which requires that the elements have controllable gains (i.e., can provide attenuation or gain to the scattered field). Such a requirement is undesirable from a cost and complexity perspective. Thus, we seek to restrict the weights such that $|w_n| = 1$. This can be written as the following minimization problem

$$\begin{aligned} \min_{\mathbf{w} \in \mathbb{C}^N} \quad & f(\mathbf{w}) = ||\mathbf{A}\mathbf{w} - \mathbf{y}||_2^2 \\ \text{s.t.} \quad & |w_n| = 1, \quad n = 1, \ldots, N, \end{aligned} \tag{11}$$

where $||\cdot||_2$ denotes the Euclidean norm. This is a non-convex, complex-valued, constant-modulus, least squares optimization problem which is a special case of non-convex quadratically-constrained quadratic programming [12]. An efficient solution is the use of Gradient Projection [14]. The details are discussed in [2] and summarized in Algorithm 1. Inside the algorithm, $\lambda_{\max}(\cdot)$ denotes the largest eigenvalue and $\angle(\cdot)$ is the phase of the element inside.

Algorithm 1 Gradient Projection.

Initialization: Set k = 0, $\alpha = \frac{1}{\lambda_{\max}(\mathbf{A}\mathbf{A}^H)}$, $\mathbf{w}^{(0)} = \mathbf{1}$.
Repeat:
$\boldsymbol{\eta}^{(k+1)} = \mathbf{w}^k - \alpha \mathbf{A}^H \left(\mathbf{A}\mathbf{w}^{(k)} - \mathbf{y}\right)$;
$\mathbf{w}^{(k+1)} = e^{\angle\left(\boldsymbol{\eta}^{(k+1)}\right)}$;
$k = k + 1$;
Until Convergence

B. Simplified method for unimodular unquantized weights

Any two complex numbers whose magnitudes sum to a value less than 2 can be replaced by two unimodular complex numbers. Additionally, in our problem the two neighboring elements in each E-field vector are nearly identical. Therefore, in cases where $||\mathbf{w}^*||_\infty \leq 1$, it is possible to replace the optimal weights $\mathbf{w}^*$ with approximately optimal unimodular weights $\tilde{\mathbf{w}}_c^*$ which satisfy $\mathbf{A}\tilde{\mathbf{w}}_c^* \approx \mathbf{A}\mathbf{w}^*$. To do this, first we replace every two adjacent columns of $\mathbf{A}$ with one column of $\tilde{\mathbf{A}}_n$ defined as

$$\tilde{\mathbf{A}}_n = (\mathbf{A}_{2n-1} + \mathbf{A}_{2n})/2, \quad n = 1, \ldots, N/2, \qquad (12)$$

where $\mathbf{A}_n$ represents the n-th column of matrix $\mathbf{A}$. Now, we require that

$$\sum_{n=1}^{\frac{N}{2}} \tilde{\mathbf{A}}_n (\tilde{w}^*_{c,2n-1} + \tilde{w}^*_{c,2n}) \approx \sum_{n=1}^{N} \mathbf{A}_n w^*_n, \qquad (13)$$

which means that for each pair of weight elements, we need

$$\tilde{\mathbf{A}}_n (\tilde{w}^*_{c,2n-1} + \tilde{w}^*_{c,2n}) \approx \mathbf{A}_{2n-1} w^*_{2n-1} + \mathbf{A}_{2n} w^*_{2n}. \qquad (14)$$

By defining $\tilde{w}_{2n-1} = e^{j\theta_1}$, $\tilde{w}_{2n} = e^{j\theta_2}$, assuming the equality can be met in equation (14), it can be re-written as

$$\begin{aligned} \cos(\theta_1) + \cos(\theta_2) &= \Re(y_n), \\ \sin(\theta_1) + \sin(\theta_2) &= \Im(y_n), \end{aligned} \qquad (15)$$

where $y_n = (\mathbf{A}_{2n-1} w^*_{2n-1} + \mathbf{A}_{2n} w^*_{2n}) \oslash \tilde{\mathbf{A}}_n$ and $\oslash$ denotes the Hadamard (element wise) division. Solving the above equation, we get

$$\theta_{1,2} = \angle(y_n) \pm \cos^{-1}\left(\frac{|y_n|}{2}\right). \qquad (16)$$

This simplified unimodular solution provides acceptable performance when compared to the optimal continuous unimodular weights $\mathbf{w}^*_c$, as we will see in section V. Importantly, since $\tilde{\mathbf{w}}^*_c$ can be written in closed form as a function of the unconstrained optimal weights $\mathbf{w}^*$, it is significantly more computationally efficient than any iterative algorithm.

C. Quantized Weights

The weights described in the previous sections have one primary disadvantage: they presume continuously-variable phase values. In a practical implementation, it is much more reasonable that only a finite number of phase values would be available on each reconfigurable element. Thus, we wish to solve the problem (11) with a new constraint that

$$\begin{aligned} \min_{\mathbf{w} \in \mathbb{C}^N} \quad & f(\mathbf{w}) = ||\mathbf{A}\mathbf{w} - \mathbf{y}||_2^2 \\ \text{s.t.} \quad & w_n \in \mathcal{W}, \quad n = 1, \ldots, N, \end{aligned} \qquad (17)$$

where $\mathcal{W} = \{w \in \mathbb{C} | w = e^{j\frac{2\pi k}{M}}, k = 0, \ldots, M-1\}$ and M is the number of possible phase values. In our previous work [2], we solved this problem via simulated annealing. Specifically, by randomly changing the phase of one weight element each time, the algorithm accepts the new weight vector if the cost is lower or accept the new weight vector with a certain probability if the cost is higher. Although the implementation is straightforward, such metaheuristic approaches have the disadvantage that their convergence rate and optimality are not guaranteed. Moreover, the lack of consistency can be problematic in applications where reproducibility is important.

A more efficient solution is to use the negative square penalty (NSP) or extreme point pursuit (EXPP) method recently proposed in [16]. Specifically, re-writing problem (17)

$$\min_{\mathbf{w} \in \bar{\mathcal{W}}^N} \quad F_c(\mathbf{w}) = ||\mathbf{A}\mathbf{w} - \mathbf{y}||_2^2 - c||\mathbf{w}||_2^2, \qquad (18)$$

where $\bar{\mathcal{W}} = \text{conv}(\mathcal{W})$ is the convex hull of $\mathcal{W}$. The authors in [17] prove that when the objective function f has a L-Lipschitz continuous gradient (L-smooth) on a convex set, problem (18) and problem (17) have the same optimal solution sets for any $c > \frac{L}{2}$, where L is defined as

$$||\nabla f(x) - \nabla f(y)||_2 \leq L||x - y||_2, \quad \forall x, y \in \mathcal{X}. \qquad (19)$$

Since our objective function is a quadratic function, L is equal to the maximum eigenvalue of $\mathbf{A}^H\mathbf{A}$.

Given that problem (18) has a convex constraint but a non-convex objective function, we can find the local optimum by leveraging the Majorize-Minimization (MM) algorithm. An optimization problem with a non-convex objective function and a convex constraint like problem (18) can be solved using algorithms that break the original problem into manageable sub-problems. For a quadratic objective function, we choose the Majorize-Minimization (MM) algorithm since it has a strong monotonicity guarantee and is more flexible in designing the surrogate function than other algorithms such as sequential convex approximation (SCA) or sequential convex programming (SCP) algorithms. Specifically, the MM algorithm is an iterative method which minimizes a series of surrogate functions of the objective function F_c. The surrogate function $g\left(\mathbf{w}\middle|\mathbf{w}^{(k)}\right)$, which is also called a majorant at the k-th step, has the properties that $g\left(\mathbf{w}\middle|\mathbf{w}^{(k)}\right) \geq F_c(\mathbf{w})$ and $g\left(\mathbf{w}^{(k)}\middle|\mathbf{w}^{(k)}\right) = F_c\left(\mathbf{w}^{(k)}\right)$ for all $\mathbf{w}$. These properties imply that optimizing the majorant will either minimize the value of F_c or leave it unchanged, therefore guaranteeing monotonic descent in the objective function at each iteration. Consequently, the solution at $(k+1)$-th step becomes

$$\mathbf{w}^{(k+1)} = \arg\min_{\mathbf{w} \in \bar{\mathcal{W}}^N} \; g\left(\mathbf{w}\middle|\mathbf{w}^{(k)}\right), \quad k = 0, 1, \ldots. \qquad (20)$$

Using the fact that $\| \mathbf{w} - \mathbf{w}^{(k)} \|_2^2 \geq 0$ for all $\mathbf{w}$ and $\mathbf{w}^{(k)}$. the majorant for F_c can be expressed as

$$\begin{aligned} F_c(\mathbf{w}) &\leq f(\mathbf{w}) - 2c\left(\mathbf{w}^{(k)}\right)^H \left(\mathbf{w} - \mathbf{w}^{(k)}\right) - c \| \mathbf{w}^{(k)} \|_2^2, \\ &= g_c\left(\mathbf{w}\middle|\mathbf{w}^{(k)}\right), \end{aligned} \qquad (21)$$

which satisfies the properties of a majorant.

Since the problem (20) is a convex problem, it can be handled by method such as the projected gradient similar to Algorithm 1 discussed in the previous section. Since $f(\mathbf{w})$ is a simple quadratic function, we use the one-step accelerated gradient projection (APG) algorithm proposed in [16]. For computational efficiency, we omit the backtracking line search step which is used to find the step size at each step k. Specifically, at k-th step, we generate an extrapolated point

$\mathbf{z}^{(k)}$ which carries the "momentum" from $\mathbf{w}^{(k)}$ and $\mathbf{w}^{(k-1)}$, then perform gradient descent at $\mathbf{z}^{(k)}$ over the majorant $g_c\left(\mathbf{z}^{(k)}\middle|\mathbf{w}^{(k)}\right)$ to find $\mathbf{z}^{(k+1)}$. Finally, we obtain $\mathbf{w}^{(k+1)}$ by projecting $\mathbf{z}^{(k+1)}$ back to the convex set $\bar{\mathcal{W}}^N$. The projection operation for the constraint of discrete phase is slightly more complicated than the case of continuous phase. Instead of solving the optimization problem of projection, the authors in [16] proposed a closed form expression of the projection:

$$\Pi_{\bar{\mathcal{W}}^N}(w) = e^{j\frac{2\pi m}{M}}\left([\Re(\bar{w})]_0^{\cos(\pi/M)} + j[\Im(\bar{w})]_{-\sin(\pi/M)}^{\sin(\pi/M)}\right), \tag{22}$$

where

$$m = \left\lfloor \frac{\angle(w) + \pi/M}{2\pi/M} \right\rfloor, \quad \bar{w} = we^{-j\frac{2\pi m}{M}}, \tag{23}$$

and $[\mathbf{w}]_{\mathbf{a}}^{\mathbf{b}}$ denotes that for each element w_n in $\mathbf{w}$

$$w_n = \min\{b_n, \max\{w_n, a_n\}\}. \tag{24}$$

Based on our empirical results, we found that the algorithm is more likely to be stuck in a poor local minimum if we choose a large penalty parameter c at the beginning. Therefore, given that our original objective function $f(\mathbf{w})$ is convex, we start with $c = 0$ and gradually increase the value to $c_{\max} > \lambda_{\max}\left(\mathbf{A}^H\mathbf{A}\right)/2$. It turns out that this strategy provides good convergence while guaranteeing that the solution will eventually lie on an extreme point which is a feasible solution for the original problem. The implementation details are provided in Algorithm 2.

Algorithm 2 Extreme Point Pursuit (EXPP).

Initialization: Set $k = 0$, $\mathbf{w}^{(-1)} = \mathbf{w}^{(0)} = \mathbf{1}$, $\xi_{-1} = 0$, $c = 0$ choose $\beta > \lambda_{\max}\left(\mathbf{A}^H\mathbf{A}\right)$ and $c_{\max} > \lambda_{\max}\left(\mathbf{A}^H\mathbf{A}\right)/2$.
Repeat:
- $\xi_k = \frac{1+\sqrt{1+4\xi_{k-1}^2}}{2}$, $\alpha_k = \frac{\xi_{k-1}-1}{\xi_k}$;
- $\mathbf{z}^{(k)} = \mathbf{w}^{(k)} + \alpha_k\left(\mathbf{w}^{(k)} - \mathbf{w}^{(k-1)}\right)$;
- $\mathbf{w}^{(k+1)} = \Pi_{\bar{\mathcal{W}}^N}\left(\mathbf{z}^{(k)} - \frac{1}{\beta}\nabla g_c\left(\mathbf{z}^{(k)}\middle|\mathbf{w}^{(k)}\right)\right)$;
- linearly increase the value of c towards $c_{\max}$, $k = k+1$;

Until Convergence

A point $\mathbf{w}$ is ϵ-stationary if

$$\operatorname{dist}(\mathbf{0}, \nabla g(\mathbf{w}) + \partial I_{\mathcal{W}}(\mathbf{w})) \le \epsilon, \tag{25}$$

where $\operatorname{dist}(\mathbf{w}, \mathcal{W}) = \inf_{\mathbf{v}\in\mathcal{W}} ||\mathbf{v}-\mathbf{w}||_2$ and $I_{\mathcal{W}}$ is the indicator function of $\mathcal{W}$. The authors in [16] show that the EXPP algorithm is guaranteed to find an ϵ-stationary point in $\mathcal{O}(1/\epsilon^2)$ iterations when $0 \le \alpha_k \le \tilde{\alpha}$, $a_1 L_g \le \beta \le a_2 L_g$ for some constants $\tilde{\alpha} = \sqrt{a_1(1-\mu)/a_2}$ with $\mu \in (0, 1]$, $a_1 \in (0, 1)$ and $a_2 \in (1, \infty)$, where L_g is the Lipschitz constant of ∇g.

IV. Limitations of Unimodular Weights

While the iterative algorithms for finding the unimodular solutions discussed above show good convergence properties, we will see that the optimal solution doesn't always provide perfect nulls for each of the desired angles. Or in other words, the unimodular solution which minimizes the squared error does not always strictly satisfy the equality in equation (7). Examining the required magnitude of the optimal weights, it's easy to show that when there is only one angle to null ($K = 1$), the condition for the existence of a unimodular solution which strictly satisfies the equality in (7) is

$$\sum_{n=1}^{N} |a_n| = ||\mathbf{A}|| \ge |y|, \tag{26}$$

where a_n is the n-th element in the vector $\mathbf{A}$, $||\cdot||$ denotes the ℓ_1 norm and y is a scalar since $K = 1$. This simply implies that energy collected from the reconfigurable surface must be larger than that obtained from the fixed portion of the surface at the desired angle ψ, a requirement also noted in section III of [1]. For the general case of $K \ge 2$, it is challenging to strictly prove the existence of a unimodular solution. However, using empirical results, we found that the existence is related to the magnitude of the elements in the unconstrained optimal weight vector. Specifically, a unimodular solution which satisfies (7) only exists when

$$\sum_{\mathcal{I}} |w_{\mathcal{I}}^*| \gtrapprox \sum_{\mathcal{J}} |w_{\mathcal{J}}^*|, \tag{27}$$

where $\mathcal{I} = \left\{n \;\middle|\; |w_n^*| \le 1\right\}$ and $\mathcal{J} = \left\{n \;\middle|\; |w_n^*| > 1\right\}$. Further, if the elements of $\mathbf{w}^*$ are sorted by increasing magnitude, with a sufficient number of elements, we can approximate the sorted vector as a linearly increasing set going from from zero to $||\mathbf{w}^*||_\infty$. Using this approximation, we can obtain a simpler criterion for determining the existence of a unimodular solution that meets the equality. Specifically, define $\epsilon = ||\mathbf{w}^*||_\infty$ meaning ϵ/N is the separation of magnitudes. By making equation (27) an equality, we obtain

$$\sum_{n=1}^{\lfloor N/\epsilon \rfloor} \frac{\epsilon}{N} n = \sum_{n=\lfloor N/\epsilon \rfloor + 1}^{N} \frac{\epsilon}{N} n, \tag{28}$$

where $\lfloor\cdot\rfloor$ denotes the floor operation. Solving and taking the non-negative solution results in

$$\epsilon = \frac{\sqrt{2N^2 + 2N + 1} + 1}{N + 1}, \qquad \lim_{N\to\infty} \epsilon = \sqrt{2}. \tag{29}$$

We will show in the next section that even though the sorted magnitude of $\mathbf{w}^*$ is not strictly linearly increasing, this threshold is accurate and allows us to quickly determine the existence of a unimodular solution which gives perfect nulls.

V. Results

To demonstrate the performance of the above algorithms, in this section we provide numerical results. The parameters of the paraboloidal reflector here are the same as those used in the Section 4 of [2]. As one typical example, the pattern in Fig. 2 is the H-plane co-pol pattern when a 2-bit discrete phase

TABLE I
AVERAGE GAIN FOR DIFFERENT ANGLES WITH MAINLOBE CONSTRAINT ($\delta = 0.01$)

Angles (degrees)	Average Gain (dBi)					$\|\|\mathbf{w}^*\|\|_\infty$
	Unconstrained $\mathbf{w}^*$	Unimodular Continuous Phase $\mathbf{w}_c^*$	Approx. Unimodular Continuous $\tilde{\mathbf{w}}_c^*$	Unimodular Discrete Phase $\mathbf{w}_d^*$ ($M = 4$)		
				EXPP	Simulated Annealing	
1.85	-315	-307	-48.77	-47.13	-48.86	0.7747
1.85, 2.05	-297	-295	-53.39	-40.56	2.96	0.8479
1.85, 2.05, 2.25	-298	-286	-22.21	-42.89	-5.80	1.1378
1.85, 2.125, 2.4, 2.675	-300	-287	-5.93	-28.15	1.10	1.3923
1.85, 2.1, 2.35, 2.6	-292	-28	-1.80	-22.92	-4.29	1.5682
1.85, 2.05, 2.25, 2.45	-296	-23	2.27	-22.17	-14.11	1.9420

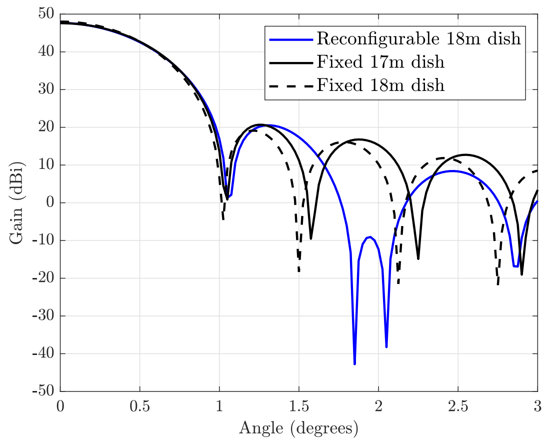

Fig. 2. H-plane co-pol pattern for traditional (fixed) 17/18m dish and reconfigurable 18m dish with 0.5m reconfigurable rim ($\psi = 1.85°, 2.05°$). The mainlobe constraint is set to $\delta = 0.01$. Discrete phase unimodular weights with $M = 4$ quantization level is applied.

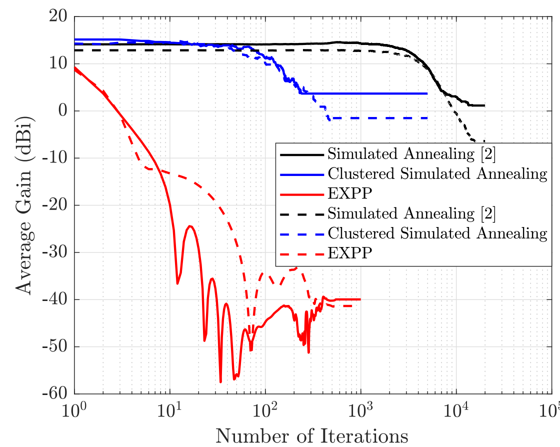

Fig. 3. Convergence rate of three different algorithms for finding the discrete phase unimodular solution. We group 2756 elements into 100 clusters for the clustered simulated annealing algorithm. The angles to be nulled are $\psi = 1.85°, 2.05°$ (solid lines) and $\psi = 1.85°, 2.05°, 2.25°$ (dashed lines). The mainlobe constraint is set to $\delta = 0.01$. Quantization level $M = 4$.

weight vector determined by the EXPP algorithm are used to place nulls at $\psi = 1.85°$ and $2.05°$ with a mainlobe constraint (within 0.01dB) applied. We can see that the gains at two the desired null angles are significantly reduced (relative to the fixed dish) and the mainlobe gain is well-maintained.

Fig. 3 compares the rate of the convergence for the EXPP algorithm as compared to the simulated annealing algorithm given in [2]. The y-axis represents the average gain at the two angles to be nulled. Note that the x-axis uses a log scale. We can see the EXPP algorithm converges to a good stationary point within 10^3 iterations while the simulated annealing algorithm takes more than 10^4 iterations to converge and does not provide a satisfactory solution. In order to achieve the same convergence rate using the metaheuristic simulated annealing algorithm, we also tried using grouped elements and updated the phase of the elements in clusters. Doing so does result in an improved convergence rate. However, the convergence rate improvement is achieved at a sacrifice in the the achievable gain. It was found that this result is representative of the behavior at other angles.

Table I presents the achievable gain at various sets of angles (rows) with different constraints (columns). As can be seen, the unconstrained optimal weights always give the perfect nulls for all desired angles. However, the continuous phase unimodular weights (found using the Gradient Projection algorithm) cannot provide perfect nulls when the number of angles is large, and the spacing between nulls is small. Referring to the last column of the table, we notice that the unimodular weights begin to provide degraded performance when the infinite norm of the unconstrained optimal weights is larger than approximately $\sqrt{2}$, which confirms the validity of our conclusion in section IV. The third column of gains corresponds to the weights generated from the approximate solution for unimodular weights given in Section III-B. In scenarios where $||\mathbf{w}^*||_\infty \leq 1$, the approximated continuous phase unimodular solution guarantees a near -50dBi gain. Given that such a gain is typically sufficient and we don't typically require perfect nulls in practice, the approximate unimodular weights deliver solid performance while possessing significantly better computational efficiency than any of the proposed iterative algorithms. Additionally, for the weights with discrete phase values, the fifth and sixth columns provide the comparison between the achievable gain obtained by the EXPP and simulated annealing. The performance of the metaheuristic algorithm is significantly reduced as we increase the number of angles to null while the EXPP algorithm still yields consistent performance.

VI. Conclusion

Motivated by the need for spectrum sharing in satellite systems, we have described multiple techniques for determining optimal or near-optimal weights for creating nulls in the pattern of a prime focus-fed circular axisymmetric paraboloidal reflector antenna equipped with a reconfigurable elements on the rim. It was shown that if the elements placed on the rim of the reflector are controlled with practical unit-modulus weights, the required weights can be found using a least-squares approach based on the projected gradient algorithm. Additionally, a closed-form solution for unimodular weights can also be found for cases where the optimal weights have an infinite norm less than or equal to unity. Further, for the case of discrete phase, a MM-based algorithm was applied to solve the transformed problem which significantly outperforms the previously proposed metaheuristic method in both the convergence rate and final gain. Finally, we explored the conditions under which a unimodular solution which strictly satisfies the linear equality exists. Specifically, unimodular weights provide excellent performance provided that the infinite norm of the optimal unconstrained weights is less than $\sqrt{2}$. This criterion also allows us to determine when a unimodular weight solution which provides nearly perfect nulls can be found using straightforward algorithms.

References

[1] S. Ellingson and R. Sengupta, "Sidelobe modification for reflector antennas by electronically reconfigurable rim scattering," *IEEE Antennas Wireless Propag. Lett.*, vol. 20, pp. 1083–1087, 2021.

[2] R. M. Buehrer and S. W. Ellingson, "Weight selection for pattern control of paraboloidal reflector antennas with reconfigurable rim scattering," in *Proc. IEEE Aerosp. Conf.*, Mar. 2023, pp. 1–8.

[3] R. Deng, B. Di, H. Zhang, L. Kuang, and L. Song, "Ultra-dense leo satellite constellations: How many leo satellites do we need?" *IEEE Trans. Wireless Commun.*, vol. 20, no. 8, pp. 4843–4857, Aug. 2021.

[4] C. Zhang, C. Jiang, L. Kuang, J. Jin, Y. He, and Z. Han, "Spatial spectrum sharing for satellite and terrestrial communication networks," *IEEE Trans. Aerosp. Electron. Syst.*, vol. 55, no. 3, pp. 1075–1089, Jun. 2019.

[5] G. Maral, M. Bousquet, and Z. Sun, *Satellite communications systems: systems, techniques and technology*. John Wiley & Sons, 2020.

[6] T. Pratt and J. E. Allnutt, *Satellite communications*. John Wiley & Sons, 2019.

[7] S. Rao, L. Shafai, and S. K. Sharma, *Handbook of Reflector Antennas and Feed Systems Volume III: Applications of Reflectors*. Artech House, 2013.

[8] W. P. Menzel and J. F. Purdom, "Introducing GOES-I: The first of a new generation of geostationary operational environmental satellites," *Bull. Amer. Meteorol. Soc.*, vol. 75, no. 5, pp. 757–782, May 1994.

[9] Y. Liu, X. Liu, X. Mu, T. Hou, J. Xu, M. Di Renzo, and N. Al-Dhahir, "Reconfigurable intelligent surfaces: Principles and opportunities," *IEEE Commun. Surveys Tuts.*, vol. 23, no. 3, pp. 1546–1577, 3rd Quart. 2021.

[10] J. Budhu, S. V. Hum, S. Ellingson, and R. M. Buehrer, "Design of rim-located reconfigurable reflectarrays for interference mitigation in reflector antennas," *IEEE Trans. Antennas Propag.*, vol. 72, no. 4, pp. 3736–3741, Apr. 2024.

[11] R. M. Buehrer and S. W. Ellingson, "Pattern control for reflector antennas using electronically-reconfigurable rim scattering," in *Proc. IEEE Int. Symp. Antennas Propag. USNC-URSI Radio Sci. Meeting (APS/URSI)*, Jul. 2022, pp. 577–578.

[12] Z. Luo, W. Ma, A. M. So, Y. Ye, and S. Zhang, "Semidefinite relaxation of quadratic optimization problems," *IEEE Signal Process. Mag.*, vol. 27, no. 3, pp. 20–34, May 2010.

[13] S. Smith, "Optimum phase-only adaptive nulling," *IEEE Trans. Signal Process.*, vol. 47, no. 7, pp. 1835–1843, Jul. 1999.

[14] J. Tranter, N. D. Sidiropoulos, X. Fu, and A. Swami, "Fast unit-modulus least squares with applications in beamforming," *IEEE Trans. Signal Process.*, vol. 65, no. 11, pp. 2875–2887, Jun. 2017.

[15] T. Vu, R. Raich, and X. Fu, "On local linear convergence of projected gradient descent for unit-modulus least squares," *IEEE Trans. Signal Process.*, vol. 71, pp. 3883–3897, Oct. 2023.

[16] M. Shao, Q. Li, W.-K. Ma, and A. M.-C. So, "A framework for one-bit and constant-envelope precoding over multiuser massive miso channels," *IEEE Trans. Signal Process.*, vol. 67, no. 20, pp. 5309–5324, Oct. 2019.

[17] J. Liu, Y. Liu, W.-K. Ma, M. Shao, and A. M.-C. So, "Extreme point pursuit–part I: A framework for constant modulus optimization," *arXiv:2403.06506*, 2024.